

# Rethinking Image Editing Detection in the Era of Generative AI Revolution

Zhihao Sun<sup>1,2</sup>, Haipeng Fang<sup>1,2</sup>, Xinying Zhao<sup>1,2</sup>, Danding Wang<sup>1,2</sup>, Juan Cao<sup>1,2</sup>

<sup>1</sup>Institute of Computing Technology, Chinese Academy of Sciences

<sup>2</sup>University of Chinese Academy of Sciences



Figure 1. GRE is a large-scale generative regional editing dataset with several distinct advantage, briefly highlighted in (b). We showcase some edited image with different editing approaches and various editing types in (a), along with their corresponding original images.

## Abstract

The accelerated advancement of generative AI significantly enhance the viability and effectiveness of generative regional editing methods. This evolution render the image manipulation more accessible, thereby intensifying the risk of altering the conveyed information within original images and even propagating misinformation. Consequently, there exists a critical demand for robust capable of detecting the edited images. However, the lack of comprehensive dataset containing images edited with abundant and advanced generative regional editing methods poses a substantial obstacle to the advancement of corresponding detection methods.

We endeavor to fill the vacancy by constructing the GRE dataset, a large-scale generative regional editing dataset with the following advantages: 1) Collection of real-world original images, focusing on two frequently edited scenarios. 2) Integration of a logical and simulated editing pipeline, leveraging multiple large models in various modalities. 3) Inclusion of various editing approaches with distinct architectures. 4) Provision of comprehensive analysis tasks. We perform comprehensive experiments with proposed three tasks: edited image classification, edited method attribution and edited region localization, providing analysis of distinct editing methods and evaluation of detection methods in related fields. We expect that the GRE

*dataset can promote further research and exploration in the field of generative region editing detection.*

## 1. Introduction

Diffusion models spark an AI generation revolution in the field of computer vision, demonstrating remarkable performance in various task scenarios such as visual content generation and controllable editing [30, 31, 48, 49]. However, the advancement of generative technologies also facilitate the dissemination of malicious fake information. While detection methods for image generation<sup>1</sup> have gathered widespread attention and research, there remains a gap in the study of generative regional editing detection.

In contrast to the challenging precise control in the full image generation techniques, local editing methods exhibit greater flexibility, which enable the modification of specific content in the original image [30, 44, 50], potentially altering the conveyed information. Moreover, compared to traditional manual manipulation using tools like PhotoShop [3], the process of generative regional editing is more convenient and user-friendly for non-professionals, while still achieving high-quality editing results. Figure 1 (a) showcases the performance of several representative generative regional editing methods, illustrating the difficulty in distinguishing between authentic and edited images. In the present day, we can indeed assert that “Seeing is not always believing.” [22] Therefore, the detection capabilities of generative regional editing merit our attention.

In this paper, we construct a novel large-scale dataset named **GRE** (Generative Regional Editing) with three tasks for generative regional editing analysis. We carefully evaluate the existing detection methods across related different domains using the GRE dataset. Extensive experiments and in-depth analysis demonstrate that this larger and more comprehensive dataset significantly enhances the development of detection methods for generative editing. Specifically, GRE dataset offers several distinct advantages over existing related datasets, which are listed below.

**(1) Real-world Original Images.** What types of images are most susceptible or frequently tampered in real world scenarios? We summarize them into two typical scenes: Daily Moment Snapshots capturing individual perspectives, and News & Public Sentiment Visuals reflecting public perspectives. For these two pivotal classes, we gather the original images for our GRE dataset. These images exhibit diversity across multiple dimensions, including objects, content and scenes, laying the foundation for the subsequent opera-

<sup>1</sup>In this paper, the term **image generation** specifically refers to instances where all pixels in an image are generated. Conversely, the term **regional editing** denotes the modification of only a portion of the pixels based on the original image, and this is also referred to as image manipulation in some related studies.

tions of abundant editing intents. Simultaneously, we place emphasis on the diversity of image resolutions within the dataset, with resolutions ranging from 480P to 2K.

**(2) Logical and Simulated Editing Pipeline.** Previously, small-scale regional editing datasets ensured logical coherence through manual manipulation, while larger datasets struggled to maintain logical consistency through naive automated editing pipeline. To ensure logical coherence in editing (*e.g.*, preventing the appearance of a dog in the sky), semantic richness in editing, data scale and scalability, we integrate multiple awesome large models in various modalities to construct a complete image editing pipeline including perception, creativity and implementation. In addition to obtaining edited images and corresponding region annotations, we document the intent behind the editing process in textual form, which serves to detection and analysis of editing intent, and enhancing interpretability and understanding of the regional editing detection.

**(3) Various Editing Approaches.** Since the remarkable performance of diffusion models [12, 33] in image generation tasks, numerous editing methods based on the principles of diffusion have emerged. While these methods share the same underlying principles, there are variations in network architecture design, editing control mechanisms, and other aspects. Whether these differences pose challenges to the generalization of region editing detection algorithms is a question worth exploring. Additionally, despite most GAN-based methods exhibit limitations in their generative capabilities, often restricted to object removal, these methods still hold value in specific scenarios. Moreover, due to the differences in principles, achieving generalization in detection for both GAN-based and diffusion-based editing methods is challenging. We select a variety of representative editing methods, including GAN-based, diffusion-based and black-box approaches, as well as different editing control mechanisms, for thorough investigation.

**(4) Comprehensive Analysis Tasks.** According to the real application scenario, we provide annotations at multiple levels and propose three tasks: 1) Edited Image Classification, distinguishes whether an image is edited or not. 3) Edited Method Attribution, identifies the editing method used in an edited image. 2) Edited Region Localization, localizes manipulated areas within edited images. The pixel-level localization task, although more challenging, is meaningful in finding edited elements within a visually rich edited image.

## 2. Related Work

### 2.1. Generation and Manipulation Datasets

**Image Generation.** Recently, there has been a growing emphasis on the detection of generative images, leading to the introduction of numerous benchmarks such as DeepArt

Dataset	Dataset Scale		Original Image		Generative Editing Approaches			Pipeline
	Edited Images	Generative Ratio(%)	Daily	News	GAN-based	Diffusion-based	Black-box	
Columbia[32]	180	0.0	✓	✗	✗	✗	✗	Random
CASIAv1[8]	920	0.0	✓	✗	✗	✗	✗	Manual
CASIAv2[8]	5,063	0.0	✓	✗	✗	✗	✗	Manual
Coverage[41]	100	0.0	✓	✗	✗	✗	✗	Manual
NIST16[10]	564	36.9	✓	✗	✓	✗	✗	Manual
DEFACTO[23]	149,587	16.7	✓	✗	✓	✗	✗	Random
IMD20[24]	2,010	0.0	✓	✗	✗	✗	✗	Manual
<b>GRE (Ours)</b>	<b>228,650</b>	<b>100.0</b>	✓	✓	✓	✓	✓	<b>Simulated</b>

Table 1. Summary of various regional editing detection datasets. GRE surpasses any other dataset both in scale and diversity. The carefully designed simulated editing pipeline is also a significant advantage.

[40], IEEE VIP Cup [38], DE-FAKE [43], and CiFAKE [5], along with the million-scale benchmark provided by Gen-Image [52]. However, the generative images within these datasets are primarily suitable for image-level generation detection tasks. They do not fully meet the requirements for the edited region localization task. Creating datasets specifically for the generative regional editing detection task incurs higher costs, and its pixel-level automated editing process is more complex compared to image-level generation.

**Regional Image Editing.** Detecting tampering or editing regions in an image is a longstanding challenge. Table 1 provides a summary of the scale, image source, and editing approaches of existing datasets, including Columbia [32], CASIA [8], Coverage [41], NIST16 [10], DEFACTO [23] and IMD20 [24], which are widely used and recognized. Among these datasets, only the DEFACTO dataset includes a relatively extensive collection of generative edited image data. Other datasets predominantly include early non-generative forms of editing (e.g., simple splice and copy-move). However, the generative editing methods employed in DEFACTO dataset are limited, and the automated editing pipeline used is relatively simple. This editing pipeline leaves noticeable traces of automation, resulting in significant generalization issues for models trained on the dataset.

## 2.2. Generative Regional Editing Methods

**Diffusion-based methods.** The emergence of diffusion models has truly propelled generative editing methods to outperform operation sequences dominated by manual interventions, both in terms of convenience and effectiveness. Stable Diffusion [30] represents an advanced text-to-image diffusion model capable. The inclusion of simple mask replacement operations during the inference process enables targeted region editing. ControlNet [50] introduces innovative modules that enable the control of pre-trained large-scale diffusion models to accommodate additional input conditions. PaintByExample [44] explores exemplar-guided image editing rather than language-guided image editing,

enabling even more precise control over the editing process.

**GAN-based methods.** However, we must also acknowledge the significant performance improvements in GAN-based image editing methods that have occurred in recent times. MAT [16] customizes an inpainting-oriented transformer block, in which the attention module aggregates non-local information exclusively from partially valid tokens, as indicated by a dynamic mask. This approach demonstrates remarkable effectiveness in addressing extensive inpainting challenges. LaMa [35] optimizes the intermediate feature maps of a network by minimizing a multi-scale consistency loss during inference. This approach adeptly handles the issue of lacking detail present at higher resolutions, resulting in improved visual quality.

## 3. GRE Construction

Most of existing image generation datasets only contain full image generated samples, without considering the common scenario of regional editing within images. Most previous regional editing datasets only contain manipulation without the participation of generative models, and the creation processes lack consideration of logical rationality and semantic diversity. On the contrast, our proposed GRE dataset provides various generative regional editing approaches, and defines three tasks (*i.e.* edited image detection, edited region localization and editing method attribution) with a total of 228K images. We design a automated editing pipeline assisted by multiple large models with different modalities, capable of performing logically consistent editing operations and recording a diverse range of editing intents. We compare our GRE with other public regional editing datasets, as detailed in Table 1. Over all the comparison items listed in the table, our dataset outperforms others in both scale and diversity.

### 3.1. Original Data Collection

In the context of the internet, we categorize images frequently selected for tampering or editing into two primary



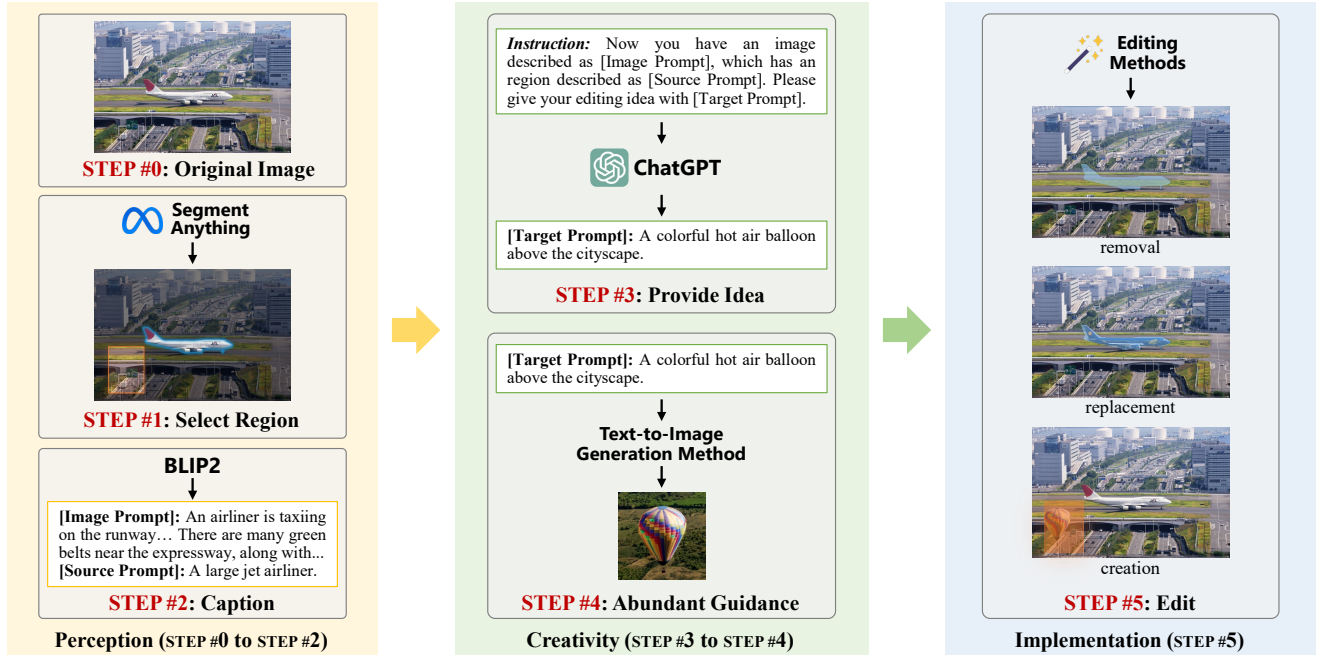


Figure 2. **Illustration of our logical and simulated pipeline for regional editing.** Simulating the real editing workflow, the process including three crucial components: **perception**, **creativity** and **implementation**. With the assistance of various large models in multiple modalities, this pipeline ensures the logical coherence and imperceptibility of editing operations.

classes: *Daily Moment Snapshots* and *News & Public Sentiment Visuals*. Building upon this conceptual framework, we gather abundant original data to enhance diversity across dimensions such as scenes, content, and resolution.

**Daily Moment Snapshots** comprises user-shared pictures capturing daily life scenes and sharing moments, depicting the ordinary and personal aspects of individuals’ lives. COCO [17] and Flickr2K [36] collected images from Flickr [2], comprising photographs uploaded by amateur photographers with searchable keywords, including 40 scene categories. Similarly, DIV2K [4] and SR-RAW [51] gathered high-resolution images from a diverse set of websites and cameras, capturing snapshots of various moments and abundant contents. We select original data from these datasets, where the resolutions range from 480P to 2K.

**News & Public Sentiment Visuals** includes visuals intricately linked to current events, news, or public sentiment, fostering broader discussions and sparking the attention of a larger audience. VisualNews [18] is a benchmark designed for the news image caption task, consisting of a large-scale collection of news images and associated metadata. The dataset was sourced from prominent news outlets such as BBC, USA Today, and The Washington Post, among others. From this dataset, we specifically select news illustrations with resolutions exceeding 720P and possessing rich content as the original images.

## 3.2. Regional Editing Pipeline

To simulate the image editing process in real-world scenarios and ensure logical coherence in edited content, we design the editing pipelines assisted by multiple large models of different modalities, as illustrated in Figure 2. This pipeline primarily consists of three pivotal components. (1) Perception, which involves selecting the region to be edited and understanding the original image content. (2) Creativity, which involves determining the editing goal, and gathering corresponding textual descriptions and image examples (the guidance inputs for subsequent editing). (3) Implementation, which entails selecting the required guidance, employing various editing methods for multiple iterations of image editing and filtering the optimal result.

### 3.2.1 Perception of Original Image

**What is the content presented in the original image?** The first crucial component of the pipeline is to achieve perception of the original image. In this component, we aim to comprehend the image and select editing regions that are diverse and reasonable for subsequent editing. In real-world scenarios, edited regions can be broadly categorized into two types: object regions and non-object regions. For the former, editing operations such as removal or replacement can be performed, while for the latter, operations involve creating content that is not present in the original image.

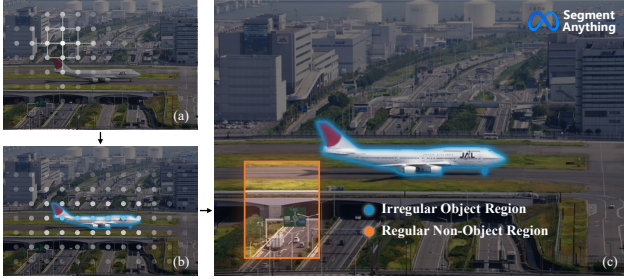


Figure 3. **Illustration of point-based SAM segmentation.** (a) Dense grid of points as the input for SAM. (b) Selection of an object if multiple points yield similar segmentation masks. (c) Outside the object region, selection of non-object regions.

To simulate the selection of objects, we employ an advanced semantic segmentation model SAM [14] to obtain precise object region masks, as illustrated in Step #1. SAM can achieve point-based segmentation. Therefore, we utilize a dense grid of points, as illustrated in Figure 3 (a), to guide SAM for multiple region predictions. For an object or region with clear semantic meaning, it should be selected by at least two points and produce similar masks. We use this criterion to filter regions with complete semantic meaning. Conversely, outside these regions, there is a high probability of being background areas with no clear semantic meaning. In these cases, we use randomly sized rectangular regions to select these areas. We employ constraints related to size and the number of connected components to eliminate fragmented and meaningless segments. Consequently, we obtain irregular object region masks and regular non-object region masks, denoted as [Region Mask], which is the most crucial guidance for subsequent editing process.

We employ the large-scale visual-text model BLIP2 [15] for the recognition of specified content in Step #2. We aim for BLIP2 to provide a detailed description of the original image, referred to as [Image Prompt]. Subsequently, we crop the selected region with bounding boxes enlarged by 1.3x. We expect BLIP2 to provide a description of the original object or content within that region, denoted as [Source Prompt]. Finally, we analyze the coarse-grained position of the selected region in the image (using combinations such as center, top, bottom, left and right) and incorporate this information with the [Source Prompt].

### 3.2.2 Creativity of Editing

**What is the idea and target of the editing?** In the real world, common editing types can be summarized as removal, replacement, and creation. Among these, removal is the most straightforward to establish, requiring only the [Region Mask] obtained in the earlier steps. However, for achieving the other editing types, the preparation of cor-

Method	Architecture	Guidance
MAT	GAN	[Region Mask]
LaMa	GAN	[Region Mask]
StableDiff	Diffusion	[Region Mask],[Target Pro.]
ControlNet	Diffusion	[Region Mask],[Target Pro.]
PaintEx	Diffusion	[Region Mask],[Target Pro.],[Target Ex.]
PhotoShop	Black-box	[Region Mask],[Target Pro.]

Table 2. The distinctive characteristics of representative generative regional editing methods.

responding guidance that can describe the editing idea and purpose becomes essential.

ChatGPT [1], developed by OpenAI upon InstructGPT [26], is an excellent advisor to generate innovative editing ideas. We utilize carefully designed instruction format<sup>2</sup> to inform ChatGPT about the content of the original image and the content of the selected region for editing. We hope that it can provide diverse and realistic editing ideas that align with real-world logic in Step #3. The required text description of the editing target, [Target Prompt], can be extracted from its response. We leverage the currently best open-source text-to-image generation model, Stable Diffusion XL [27], to translate the text description into image examples [Target Example] in Step #4. This serves as a different form of guidance needed for the subsequent editing process. It’s essential to clarify that the target examples generated in this step do not belong to the final dataset, they are merely the guidance generated by the intermediate steps.

The potential improvement of editing detection performance through the incorporation of editing intent is worthwhile investigation. Considering that existing datasets do not annotate the editing intent for each edited image, we aim for ChatGPT to leverage the previously obtained [Image Prompt],[Source Prompt], and [Target Prompt] to analyze the intent behind each editing task. Subsequently, this [Editing Intent] is utilized as an annotation for each edited image.

### 3.3. Various Generative Regional Editing Methods

We have gathered comprehensive guidance information for region editing, including a precise binary mask indicating the editing region [Region Mask], textual descriptions indicating the editing target [Target Prompt], and image examples providing visual references for the editing target [Target Example]. These pieces of information offer diverse guidance for generative region editing methods, enabling end-to-end region editing.

<sup>2</sup>**Instruction Format:** Now you have an image described as image prompt: [Image Prompt], which has an region described as source prompt: [Source Prompt]. This area may be an object or an empty background area. Now you need to edit or tamper with this area. You can make creative edits out of fun, or you can change the original meaning of this image out of any intent. Please give your editing ideas and describe the expected target of this region as target prompt: [Target Prompt].

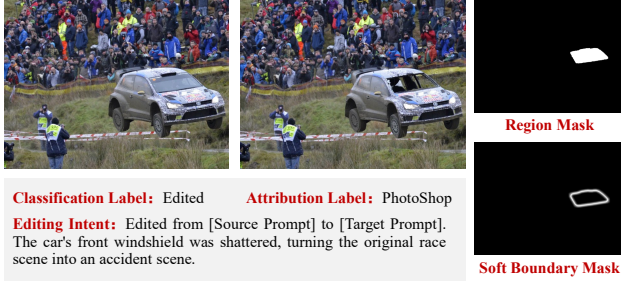


Figure 4. Examples showcasing the rich provided annotations.

Some works in image generation detection and attribution proposed and analyzed various generative methods from different perspectives, highlighting that different methods leave distinct traces and fingerprints [46]. Moreover, there is a noted poor generalization of detection models across data generated by different methods. To ensure diversity in edited images within our GRE dataset and to provide a reasonable benchmark for generalization evaluation, we have chosen six editing methods to complete the final component in the pipeline, implementation. These six editing methods include MAT, LaMa, Stable Diffusion V2.0 (SD-V2.0), ControlNet, PaintByExample (PaintEx), and PhotoShop, which has introduced Generative AI functionality. Their characteristics are summarized in Table 2.

For each original image, we employ all white-box methods to generate corresponding edited images. However, due to the manual intervention required in the generative editing process within PhotoShop, we select only a subset of images for PhotoShop editing. When using the three diffusion models in the above-mentioned editing methods, we incorporate diverse inference steps, randomly selecting the number of steps from the set [20, 30, 50, 100] for each inference. Considering the variable quality of images generated by the diffusion-based model, multiple images are generated for each case. Subsequently, we choose the image with higher textual faithfulness based on the CLIP score [29]. Finally, we simulate real-world scenarios by introducing perturbations to the edited images, involving random combinations of different compression algorithms and noise addition algorithms, among other post-processing operations.

### 3.4. Annotations

For each image in the GRE dataset, we provide multiple annotations, including a 2-way classification label (authentic or edited), an  $n$ -way classification label for the image (authentic or specific editing methods), and a binary segmentation mask (authentic region or edited region).

Furthermore, compared to the original images, all edited images have additional annotations shown as Figure 4. After each editing operation, we obtain a textual description [Intent Description] of the editing intent sum-

marized by ChatGPT. Several methods in the field of image tampering detection have validated that supervision on the boundaries of edited regions can enhance detection performance. Therefore, inspired by the boundary sliding mechanism in SAFL-Net [34], we derived soft boundary masks.

## 4. Generative Regional Editing Analysis

### 4.1. Evaluation on GRE Benchmark

#### 4.1.1 Benchmark Settings

**Dataset Partition.** For each original image collected in GRE, we employ all white-box methods to generate corresponding edited images, resulting in a dataset with a distribution from 1 (authentic) to  $n$  (edited). Consequently, we group images edited with the same method into a subset, while all original images formed the authentic subset. To ensure data uniformity and prevent data leakage, we initially partition the subset of authentic images into training, validation, and test sets in ratio of 8 : 1 : 1. the division of each edited subset remains consistent with the authentic subset. In other words, if an original image is in the test set, all images edited from it also belong to the test set, ensuring exclusion from the training set.

**Task 1. Edited Image Classification.** This corresponds to a 2-ways image-level classification task designed for distinguishing between authentic and edited images. We design the evaluation protocol to analyze the distinctions among various editing methods and assess the generalization performance of different detection methods in image generation detection. For the binary classification task, we evaluate with Accuracy as the metric.

- **Protocol:** Training on the combination of authentic and one edited subset, and tested on other edited subsets.

**Task 2. Edited Method Attribution.** This refers to a  $n$ -ways (authentic and  $n - 1$  editing methods) model-level attribution task. Beyond discerning between authentic and edited images, the objective is to attribute edited images to the specific editing method employed. Evaluation metrics include Accuracy, F1-score and mean Average Precision.

- **Protocol:** All the authentic and edited subsets are used for training, while the test set is reserved for evaluation.

**Task 3. Edited Region Localization.** This concerns a 2-ways pixel-level segmentation task designed to distinguish between authentic and edited regions in images. For a comprehensive analysis, we introduce two protocols to analysis different editors and evaluate the existing manipulation localization methods, utilizing Intersection over Union (IoU) and F1-score as assessment metrics.

- **Protocol 1:** Training on one arbitrary edited subset and tested on the other edited subsets. The authentic subset is not used since both authentic and edited regions are present within the edited subset.



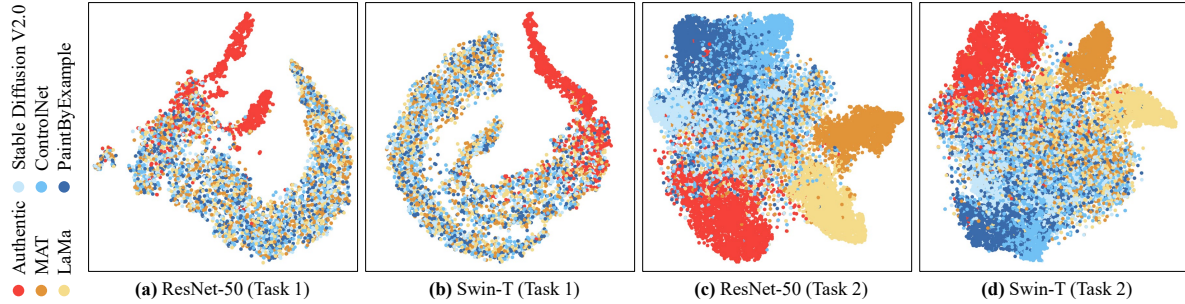


Figure 5. The t-SNE feature visualization of the authentic images and images edited by different regional editing approaches. The ResNet-50 and Swin-T are trained with protocol in Task 1 and Task 2 respectively.

Training Subset	Testing Subset (Accuracy)					
	Authentic	MAT	LaMa	SD-V2.0	ControlNet	PaintEx
MAT	92.2	88.5	89.1	85.9	86.3	85.8
LaMa	91.9	89.9	90.0	87.7	88.1	87.4
StableDiff	90.7	91.1	91.3	88.5	88.1	88.3
ControlNet	86.9	93.6	94.0	92.4	91.4	91.5
PaintEx	92.4	86.1	85.3	83.4	83.9	82.6

Table 3. **Edited Image Classification (Task 1).** The cross-editors evaluation of ResNet-50. The authentic subset and specific subset listed in *Training Subset* are used for training.

Method	Seen Subset		Unseen Subset			
	Authentic	SD-V2.0	MAT	LaMa	ControlNet	PaintEx
ResNet-18	89.8	86.5	79.4	80.6	81.1	81.9
ResNet-50	90.7	88.5	91.1	<b>91.3</b>	88.1	88.3
DeiT-S	91.6	79.3	72.0	73.8	71.9	71.5
Swin-T	<b>95.4</b>	87.8	85.5	85.6	86.1	85.2
CNNSpot	85.8	73.6	71.3	72.9	70.7	69.5
F3Net	82.3	68.1	62.4	61.7	59.8	60.5
GramNet	92.7	<b>93.2</b>	91.5	90.7	89.0	88.9
Universal	91.0	93.1	<b>91.9</b>	91.2	<b>91.5</b>	<b>91.4</b>

Table 4. **Edited Image Classification (Task 1).** The Evaluation of various classification methods. The authentic subset and SD-V2.0 subset are used for training. The metric is Accuracy.

- **Protocol 2:** Training using a combination of the MAT subset and SD-V2.0 subset, followed by testing on other subsets. The combined training set includes one GAN-based and diffusion-based editing method respectively, providing a more comprehensive assessment for image manipulation localization methods.

#### 4.1.2 Edited Image Classification

In the setting of Task 1, we chose ResNet-50 [11] as the baseline model and evaluated its performance across diverse editing subsets, as shown in Table 3. Notably, the baseline model exhibits commendable generalization performance when tested on unseen subsets. There is no significant difference observed among different editing methods. Therefore, we choose the authentic subset and SD-V2.0 subset as the training sets and conduct the evaluation.

True Label	ResNet-18						ResNet-50					
	Authentic	MAT	LaMa	SD-V2.0	ControlNet	PaintEx	Authentic	MAT	LaMa	SD-V2.0	ControlNet	PaintEx
Authentic	0.49	0.07	0.09	0.20	0.08	0.08	0.66	0.03	0.03	0.12	0.07	0.09
MAT	0.01	0.58	0.10	0.21	0.07	0.03	0.01	0.73	0.06	0.13	0.06	0.02
LaMa	0.01	0.04	0.65	0.21	0.06	0.03	0.01	0.03	0.79	0.11	0.04	0.02
SD-V2.0	0.01	0.04	0.08	0.70	0.11	0.06	0.02	0.02	0.04	0.78	0.08	0.05
ControlNet	0.01	0.03	0.07	0.36	0.43	0.09	0.01	0.02	0.03	0.23	0.63	0.08
PaintEx	0.01	0.02	0.04	0.30	0.18	0.45	0.01	0.01	0.01	0.18	0.18	0.61

Figure 6. **Edited Method Attribution (Task 2).** The confusion matrix of ResNet-18 and ResNet-50.

For comprehensive evaluation, we provide results of several baseline models, including ResNet-18 [11], ResNet-50 [11], DeiT-S [37] and Swin-T [21]. We extend SOTA detection methods for image generation detection to the classification task of regional editing images. It is observed that the performance of GramNet [20] and Universal [25] surpasses that of CNNSpot [39], F3Net [28] and baseline. However, in Figure 5 (a) and (b), we utilize t-SNE to analyze and visualize the features of two baselines, ResNet-50 and Swin-T. An evident observation from Table 4 emerges, while the features of authentic images and edited images form a distinct classification boundary, the features of images edited using different methods do not cluster well.

#### 4.1.3 Editing Method Attribution

We expand the 2-way classification labels of Task 1 to  $n$ -way attribution labels in Task 2. In addition to distinguishing between authentic and edited images, our objective is to attribute edited images to the specific editing method employed. Following the protocol in Task 2, we use the authentic subset and all edited subsets for both training and testing, constituting a closed-set attribution task.

In addition to the classification baselines mentioned earlier, we also evaluate SOTA attribution models, including DCT-CNN [9], DNA-Det [45], RepMix [6], and POSE [47]. The experimental results are presented in Table 5. We also

Method	Accuracy	F1-score	mAP
ResNet-18	64.2	67.5	76.7
ResNet-50	72.6	73.4	82.8
Deit-S	61.9	66.0	71.4
Swin-T	<b>74.3</b>	74.7	82.1
DCT-CNN	67.4	67.1	78.2
DNA-Det	72.8	74.5	82.0
RepMix	72.5	73.9	<b>83.6</b>
POSE	74.1	<b>75.8</b>	83.1

Table 5. **Edited Method Attribution (Task 2)**. The Evaluation of various attribution methods. All the authentic and edited subsets in the training set are used for training.

employ t-SNE to visualize the feature distributions of two baselines (ResNet-50 and Swin-T) under the protocol of Task 2, as shown in Figures 5 (c) and (d). Through comparison with Figures 5 (a) and (b), a crucial change is observed, where images edited by different methods cluster more distinctly. Additionally, various GAN-based methods can be well distinguished, while distinction among different diffusion-based methods is more challenging. Furthermore, in Figure 6, we present the confusion matrices for the attribution results of ResNet-18 and ResNet-50, aligning with the observation mentioned earlier.

#### 4.1.4 Edited Region Localization

In the context regional edited images detection, merely distinguishing between authentic and edited images is insufficient. Locating the edited regions is a core task, and it is also the most challenging. Following the setting of *Protocol 1* in Task 3, we choose Unet with EfficientNet-B4 as backbone (abbreviated as Unet-Eb4) as the baseline model and test its generalization performance across diverse editing subsets, as shown in Table 6. Specifically, the baseline method demonstrates acceptable localization abilities within the seen editing subset, but its generalization capabilities significantly decrease when tested on unseen subsets. An crucial observation is that the generalization difficulty among methods with different architectures (GAN-based and diffusion-based) surpasses that between methods with the same architecture. Therefore, we design *Protocol 2* for a more comprehensive and fair analysis.

To establish a comprehensive evaluation, we select classic baselines and representative image manipulation detection methods. We employ different combinations of classic segmentation models (Unet and Deeplab<sub>v3</sub>) and backbones (ResNet-50 and EfficientNet-B4) as baselines for the segmentation task. For Mantra-Net [42] and SPAN [13], the core lies in their pre-trained feature extractor. Therefore, we did not retrain them on GRE training set but rather evaluated their pre-trained models on testing set, which is indicated by the asterisk. In addition, we evaluate MVSS-Net [7], PSCC-Net [19] and SAFL-Net [34] according to *Protocol 2*. The detailed experiments are presented in Table 7.

Training Subset	Testing Subset (IoU / F1)				
	MAT	LaMa	SD-V2.0	ControlNet	PaintEx
MAT	<u>76.1/85.0</u>	27.7/36.9	2.8/4.4	7.1/10.6	4.4/6.7
LaMa	26.0/35.9	<u>76.8/84.9</u>	1.9/3.0	3.0/4.8	1.5/2.5
StableDiff	15.2/21.4	11.2/16.2	<u>57.9/67.1</u>	42.5/50.5	53.2/62.1
ControlNet	15.2/22.3	5.6/8.7	21.8/28.2	<u>70.1/78.2</u>	63.9/72.9
PaintEx	13.9/19.7	6.0/9.0	33.4/41.1	62.1/70.2	<u>76.3/84.1</u>

Table 6. **Edited Region Localization (Task 3, Protocol 1)**. The results of Unet with EfficientNet-B4 as backbone trained on different training subsets and evaluated on different testing subsets.

Method	Seen Subset		Unseen Subset		
	MAT	SD-V2.0	LaMa	ControlNet	PaintEx
Unet-R50	72.0/80.4	57.9/66.1	29.9/38.0	54.7/62.9	62.5/70.9
Unet-Eb4	76.3/84.7	65.1/74.1	40.5/50.7	60.2/69.1	66.5/75.5
Deeplab <sub>v3</sub> -R50	72.6/81.4	61.1/70.2	38.6/48.2	59.4/68.4	64.8/73.9
Deeplab <sub>v3</sub> -Eb4	78.1/87.9	59.8/69.5	38.4/47.6	54.0/64.5	60.4/70.6
Mantra-Net*	-	-	0.1/0.1	0.1/0.1	0.1/0.1
SPAN*	-	-	0.1/0.1	0.1/0.2	0.1/0.1
PSCC-Net	38.9/50.0	26.6/37.1	17.4/25.1	25.3/35.8	26.9/35.5
MVSS-Net	63.7/73.1	47.6/56.8	25.9/33.4	45.2/54.0	52.6/62.2
SAFL-Net	75.7/84.2	58.9/64.6	35.6/41.1	61.0/67.5	65.4/74.9

Table 7. **Edited Region Localization (Task 3, Protocol 2)**. The results of different methods trained on the combination of MAT subset and SD-V2.0 subset. IoU and F1-score are reported.

It is worth noting that all methods exhibit acceptable localization abilities within the seen subsets. However, there is a notable lack of generalization within the unseen subsets. An important factor contributing to this phenomenon is that these methods primarily focus on non-generative forms of region editing (e.g., simple splice and copy-move). In contrast, generative regional editing approaches produce higher-quality images with less distinct boundary for edited regions. The logic and simulated characteristics of our editing pipeline further ensure that editing operations are less perceptible. This emphasizes the value of our proposed GRE dataset for the field of regional editing detection.

## 5. Conclusion

We construct GRE, a novel and expansive benchmark designed for generative regional editing detection and analysis. Compared with existing datasets for regional editing detection, GRE stands out by curating a diverse collection of real-world images, designing a simulated editing pipeline, and including a variety of generative regional editing approaches. We also introduce three practical applications, including edited image classification, edited method attribution, and edited region localization, providing a comprehensive analysis of regional editing within the context of emerging scenarios. Our future work involves continually enriching GRE by incorporating new editing methods and novel large models into our pipeline. We aim for GRE to foster innovation and progress in this evolving field.



## References

- [1] Openai chatgpt. <https://chat.openai.com>. 5
- [2] Flickr. <https://www.flickr.com>. 4
- [3] Adobe photoshop. <https://www.adobe.com/products/photoshop.html>. 2
- [4] Eirikur Agustsson and Radu Timofte. Ntire 2017 challenge on single image super-resolution: Dataset and study. In *Proceedings of the IEEE conference on computer vision and pattern recognition workshops*, pages 126–135, 2017. 4
- [5] Jordan J Bird and Ahmad Lotfi. Cifake: Image classification and explainable identification of ai-generated synthetic images. *arXiv preprint arXiv:2303.14126*, 2023. 3
- [6] Tu Bui, Ning Yu, and John Collomosse. Repmix: Representation mixing for robust attribution of synthesized images. In *European Conference on Computer Vision*, pages 146–163. Springer, 2022. 7
- [7] Xinru Chen, Chengbo Dong, Jiaqi Ji, Juan Cao, and Xirong Li. Image manipulation detection by multi-view multi-scale supervision. In *Proceedings of the IEEE/CVF International Conference on Computer Vision*, pages 14185–14193, 2021. 8
- [8] Jing Dong, Wei Wang, and Tieniu Tan. Casia image tampering detection evaluation database. In *2013 IEEE China Summit and International Conference on Signal and Information Processing*, pages 422–426. IEEE, 2013. 3
- [9] Joel Frank, Thorsten Eisenhofer, Lea Schönherr, Asja Fischer, Dorothea Kolossa, and Thorsten Holz. Leveraging frequency analysis for deep fake image recognition. In *International conference on machine learning*, pages 3247–3258. PMLR, 2020. 7
- [10] Haiying Guan, Mark Kozak, Eric Robertson, Yooyoung Lee, Amy N Yates, Andrew Delgado, Daniel Zhou, Timothee Kheyrkhan, Jeff Smith, and Jonathan Fiscus. Mfc datasets: Large-scale benchmark datasets for media forensic challenge evaluation. In *2019 IEEE Winter Applications of Computer Vision Workshops (WACVW)*, pages 63–72. IEEE, 2019. 3
- [11] Kaiming He, Xiangyu Zhang, Shaoqing Ren, and Jian Sun. Deep residual learning for image recognition. In *Proceedings of the IEEE conference on computer vision and pattern recognition*, pages 770–778, 2016. 7
- [12] Jonathan Ho, Ajay Jain, and Pieter Abbeel. Denoising diffusion probabilistic models. pages 6840–6851, 2020. 2
- [13] Xuefeng Hu, Zhihan Zhang, Zhenye Jiang, Syomantak Chaudhuri, Zhenheng Yang, and Ram Nevatia. Span: Spatial pyramid attention network for image manipulation localization. In *European conference on computer vision*, pages 312–328. Springer, 2020. 8
- [14] Alexander Kirillov, Eric Mintun, Nikhila Ravi, Hanzi Mao, Chloe Rolland, Laura Gustafson, Tete Xiao, Spencer Whitehead, Alexander C Berg, Wan-Yen Lo, et al. Segment anything. *arXiv preprint arXiv:2304.02643*, 2023. 5
- [15] Junnan Li, Dongxu Li, Silvio Savarese, and Steven Hoi. Blip-2: Bootstrapping language-image pre-training with frozen image encoders and large language models. *arXiv preprint arXiv:2301.12597*, 2023. 5
- [16] Wenbo Li, Zhe Lin, Kun Zhou, Lu Qi, Yi Wang, and Ji-aya Jia. Mat: Mask-aware transformer for large hole image inpainting. In *Proceedings of the IEEE/CVF conference on computer vision and pattern recognition*, pages 10758–10768, 2022. 3
- [17] Tsung-Yi Lin, Michael Maire, Serge Belongie, James Hays, Pietro Perona, Deva Ramanan, Piotr Dollár, and C Lawrence Zitnick. Microsoft coco: Common objects in context. In *European conference on computer vision*, pages 740–755. Springer, 2014. 4
- [18] Fuxiao Liu, Yinghan Wang, Tianlu Wang, and Vicente Ordonez. Visual news: Benchmark and challenges in news image captioning. *arXiv preprint arXiv:2010.03743*, 2020. 4
- [19] Xiaohong Liu, Yaojie Liu, Jun Chen, and Xiaoming Liu. Psc-net: Progressive spatio-channel correlation network for image manipulation detection and localization. *IEEE Transactions on Circuits and Systems for Video Technology*, 32(11):7505–7517, 2022. 8
- [20] Zhengzhe Liu, Xiaojuan Qi, and Philip HS Torr. Global texture enhancement for fake face detection in the wild. In *Proceedings of the IEEE/CVF conference on computer vision and pattern recognition*, pages 8060–8069, 2020. 7
- [21] Ze Liu, Yutong Lin, Yue Cao, Han Hu, Yixuan Wei, Zheng Zhang, Stephen Lin, and Baining Guo. Swin transformer: Hierarchical vision transformer using shifted windows. In *Proceedings of the IEEE/CVF international conference on computer vision*, pages 10012–10022, 2021. 7
- [22] Zeyu Lu, Di Huang, Lei Bai, Xihui Liu, Jingjing Qu, and Wanli Ouyang. Seeing is not always believing: A quantitative study on human perception of ai-generated images. *arXiv preprint arXiv:2304.13023*, 2023. 2
- [23] Gaël Mahfoudi, Badr Tajini, Florent Retraint, Frederic Morain-Nicolier, Jean Luc Dugelay, and PIC Marc. Defacto: image and face manipulation dataset. In *2019 27th european signal processing conference (EUSIPCO)*, pages 1–5. IEEE, 2019. 3
- [24] Adam Novozamsky, Babak Mahdian, and Stanislav Saic. Imd2020: a large-scale annotated dataset tailored for detecting manipulated images. In *Proceedings of the IEEE/CVF Winter Conference on Applications of Computer Vision Workshops*, pages 71–80, 2020. 3
- [25] Utkarsh Ojha, Yuheng Li, and Yong Jae Lee. Towards universal fake image detectors that generalize across generative models. In *Proceedings of the IEEE/CVF Conference on Computer Vision and Pattern Recognition*, pages 24480–24489, 2023. 7
- [26] Long Ouyang, Jeffrey Wu, Xu Jiang, Diogo Almeida, Carroll Wainwright, Pamela Mishkin, Chong Zhang, Sandhini Agarwal, Katarina Slama, Alex Ray, et al. Training language models to follow instructions with human feedback. *Advances in Neural Information Processing Systems*, 35:27730–27744, 2022. 5
- [27] Dustin Podell, Zion English, Kyle Lacey, Andreas Blattmann, Tim Dockhorn, Jonas Müller, Joe Penna, and Robin Rombach. Sdxl: Improving latent diffusion models for high-resolution image synthesis. *arXiv preprint arXiv:2307.01952*, 2023. 5
- [28] Yuyang Qian, Guojun Yin, Lu Sheng, Zixuan Chen, and Jing Shao. Thinking in frequency: Face forgery detection by min-

- ing frequency-aware clues. In *European conference on computer vision*, pages 86–103. Springer, 2020. 7
- [29] Alec Radford, Jong Wook Kim, Chris Hallacy, Aditya Ramesh, Gabriel Goh, Sandhini Agarwal, Girish Sastry, Amanda Askell, Pamela Mishkin, Jack Clark, et al. Learning transferable visual models from natural language supervision. In *International conference on machine learning*, pages 8748–8763. PMLR, 2021. 6
- [30] Robin Rombach, Andreas Blattmann, Dominik Lorenz, Patrick Esser, and Björn Ommer. High-resolution image synthesis with latent diffusion models. In *Proceedings of the IEEE/CVF conference on computer vision and pattern recognition*, pages 10684–10695, 2022. 2, 3
- [31] Chitwan Saharia, William Chan, Saurabh Saxena, Lala Li, Jay Whang, Emily L Denton, Kamyar Ghasemipour, Raphael Gontijo Lopes, Burcu Karagol Ayan, Tim Salimans, et al. Photorealistic text-to-image diffusion models with deep language understanding. *Advances in Neural Information Processing Systems*, 35:36479–36494, 2022. 2
- [32] Jianbo Shi and Jitendra Malik. Normalized cuts and image segmentation. *IEEE Transactions on pattern analysis and machine intelligence*, 22(8):888–905, 2000. 3
- [33] Yang Song, Jascha Sohl-Dickstein, Diederik P Kingma, Abhishek Kumar, Stefano Ermon, and Ben Poole. Score-based generative modeling through stochastic differential equations. 2020. 2
- [34] Zhihao Sun, Haoran Jiang, Danding Wang, Xirong Li, and Juan Cao. Saf-net: Semantic-agnostic feature learning network with auxiliary plugins for image manipulation detection. In *Proceedings of the IEEE/CVF International Conference on Computer Vision*, pages 22424–22433, 2023. 6, 8
- [35] Roman Suvorov, Elizaveta Logacheva, Anton Mashikhin, Anastasia Remizova, Arsenii Ashukha, Aleksei Silvestrov, Naejin Kong, Harshith Goka, Kiwoong Park, and Victor Lempitsky. Resolution-robust large mask inpainting with fourier convolutions. In *Proceedings of the IEEE/CVF winter conference on applications of computer vision*, pages 2149–2159, 2022. 3
- [36] Radu Timofte, Eirikur Agustsson, Luc Van Gool, Ming-Hsuan Yang, and Lei Zhang. Ntire 2017 challenge on single image super-resolution: Methods and results. In *Proceedings of the IEEE conference on computer vision and pattern recognition workshops*, pages 114–125, 2017. 4
- [37] Hugo Touvron, Matthieu Cord, Matthijs Douze, Francisco Massa, Alexandre Sablayrolles, and Hervé Jégou. Training data-efficient image transformers & distillation through attention. In *International conference on machine learning*, pages 10347–10357. PMLR, 2021. 7
- [38] Luisa Verdoliva, Davide Cozzolino, and Koki Nagano. 2022 ieeecv image and video processing cup synthetic image detection. 3
- [39] Sheng-Yu Wang, Oliver Wang, Richard Zhang, Andrew Owens, and Alexei A Efros. Cnn-generated images are surprisingly easy to spot... for now. In *Proceedings of the IEEE/CVF conference on computer vision and pattern recognition*, pages 8695–8704, 2020. 7
- [40] Yabin Wang, Zhiwu Huang, and Xiaopeng Hong. Benchmarking deepart detection. *arXiv preprint arXiv:2302.14475*, 2023. 3
- [41] Bihan Wen, Ye Zhu, Ramanathan Subramanian, Tian-Tsong Ng, Xuanjing Shen, and Stefan Winkler. Coverage—a novel database for copy-move forgery detection. In *2016 IEEE international conference on image processing (ICIP)*, pages 161–165. IEEE, 2016. 3
- [42] Yue Wu, Wael AbdAlmageed, and Premkumar Natarajan. Mantra-net: Manipulation tracing network for detection and localization of image forgeries with anomalous features. In *Proceedings of the IEEE/CVF Conference on Computer Vision and Pattern Recognition*, pages 9543–9552, 2019. 8
- [43] Qiang Xu, Hao Wang, Laijin Meng, Zhongjie Mi, Jianye Yuan, and Hong Yan. Exposing fake images generated by text-to-image diffusion models. *Pattern Recognition Letters*, 2023. 3
- [44] Binxin Yang, Shuyang Gu, Bo Zhang, Ting Zhang, Xuejin Chen, Xiaoyan Sun, Dong Chen, and Fang Wen. Paint by example: Exemplar-based image editing with diffusion models. In *Proceedings of the IEEE/CVF Conference on Computer Vision and Pattern Recognition*, pages 18381–18391, 2023. 2, 3
- [45] Tianyun Yang, Ziyao Huang, Juan Cao, Lei Li, and Xirong Li. Deepfake network architecture attribution. In *Proceedings of the AAAI Conference on Artificial Intelligence*, pages 4662–4670, 2022. 7
- [46] Tianyun Yang, Juan Cao, Danding Wang, and Chang Xu. Fingerprints of generative models in the frequency domain. *arXiv preprint arXiv:2307.15977*, 2023. 6
- [47] Tianyun Yang, Danding Wang, Fan Tang, Xinying Zhao, Juan Cao, and Sheng Tang. Progressive open space expansion for open-set model attribution. In *Proceedings of the IEEE/CVF Conference on Computer Vision and Pattern Recognition*, pages 15856–15865, 2023. 7
- [48] Jiahui Yu, Yuanzhong Xu, Jing Yu Koh, Thang Luong, Gunjan Baid, Zirui Wang, Vijay Vasudevan, Alexander Ku, Yinfei Yang, Burcu Karagol Ayan, et al. Scaling autoregressive models for content-rich text-to-image generation. *arXiv preprint arXiv:2206.10789*, 2(3):5, 2022. 2
- [49] Han Zhang, Weichong Yin, Yewei Fang, Lanxin Li, Boqiang Duan, Zhihua Wu, Yu Sun, Hao Tian, Hua Wu, and Haifeng Wang. Ernie-vilg: Unified generative pre-training for bidirectional vision-language generation. *arXiv preprint arXiv:2112.15283*, 2021. 2
- [50] Lvmin Zhang and Maneesh Agrawala. Adding conditional control to text-to-image diffusion models. *arXiv preprint arXiv:2302.05543*, 2023. 2, 3
- [51] Xuaner Zhang, Qifeng Chen, Ren Ng, and Vladlen Koltun. Zoom to learn, learn to zoom. In *Proceedings of the IEEE/CVF Conference on Computer Vision and Pattern Recognition*, pages 3762–3770, 2019. 4
- [52] Mingjian Zhu, Hanting Chen, Qiangyu Yan, Xudong Huang, Guanyu Lin, Wei Li, Zhijun Tu, Hailin Hu, Jie Hu, and Yunhe Wang. Genimage: A million-scale benchmark for detecting ai-generated image. *arXiv preprint arXiv:2306.08571*, 2023. 3